Developmental Biology **251,** 320–332 (2002)
doi:10.1006/dbio.2002.0811

Mouse GLI3 Regulates *Fgf8* Expression and Apoptosis in the Developing Neural Tube, Face, and Limb Bud

Kazushi Aoto,*,† Tamiko Nishimura,* Kazuhiro Eto,† and Jun Motoyama*,[1]

**Molecular Neuropathology Group, Brain Science Institute, The Institute of Physical and Chemical Research (RIKEN), 2-1 Hirosawa, Wako, Saitama 351-0198, Japan; and †Department of Molecular Craniofacial Embryology, Graduate School of Tokyo Medical and Dental University, 1-5-45 Yushima, Bunkyo-ku, Tokyo 113-8549, Japan*

The zinc finger transcription factor GLI3 is considered a repressor of vertebrate Hedgehog (Hh) signaling. In humans, the absence of GLI3 function causes Greig cephalopolysyndactyly syndrome, affecting the development of the brain, eye, face, and limb. Because the etiology of these malformations is not well understood, we examined the phenotype of mouse *Gli3*$^{-/-}$ mutants as a model to investigate this. We observed an up-regulation of *Fgf8* in the anterior neural ridge, isthmus, eye, facial primordia, and limb buds of mutant embryos, sites coinciding with the human disease. Intriguingly, endogenous apoptosis was reduced in *Fgf8*-positive areas in *Gli3*$^{-/-}$ mutants. Since SHH is thought to be involved in *Fgf8* regulation, we compared *Fgf8* expression in *Shh*$^{-/-}$ and *Gli3*$^{-/-}$;*Shh*$^{-/-}$ mutant embryos. Whereas *Fgf8* expression was almost absent in *Shh*$^{-/-}$ mutants, it was up-regulated in *Gli3*$^{-/-}$;*Shh*$^{-/-}$ double mutants, suggesting that SHH is not required for *Fgf8* induction, and that GLI3 normally represses *Fgf8* independently of SHH. In the limb bud, we provide evidence that ectopic expression of *Gremlin* in *Gli3*$^{-/-}$ mutants might contribute to a decrease in apoptosis. Together, our data reveal that GLI3 limits *Fgf8*-expression domains in multiple tissues, through a mechanism that may include the induction or maintenance of apoptosis.

Key Words: **GLI3; FGF8; SHH; brain patterning; optic field; limb development; facial malformation; apoptosis.**

INTRODUCTION

The Hedgehog (Hh) signaling cascade is essential for many aspects of mammalian embryogenesis, including neural tube, face, limb, hair, tooth, and gut development (Chiang *et al.*, 1996). Much remains to be learned about the signaling cascade in both *Drosophila*, in which pioneering work has been done, and vertebrates (Ingham and McMahon, 2001). In *Drosophila*, Hh acts as a secreted signaling protein that inhibits the transmembrane receptor Patched (Ptc) (Ingham, 1998). In the absence of Hh, Ptc inhibits the activity of a second transmembrane protein, Smoothened (Smo), thereby blocking the downstream signaling cascade. Hh binding inactivates Ptc, releasing Smo to activate downstream genes. Smo appears to affect a cytoplasmic protein complex that includes the zinc finger transcription factor Cubitus interruptus (Ci) (Methot and Basler, 2001). Smo activity leads to the formation of Ci as a transcriptional activator. When Hh is absent and Ptc prevails over Smo, Ci is proteolytically processed into a transcriptional repressor form. Vertebrate homologs of Hh (Desert hedgehog, Indian hedgehog, and Sonic hedgehog), Ptc (Ptc1 and 2), Smo, and Ci (Gli1, 2, and 3) have been identified and seem to act in a signaling cascade similar to that characterized in *Drosophila*. Numerous functions of the vertebrate Hedgehog signals have been identified, in a multitude of tissues.

The Gli zinc finger proteins seem to play a central role in the mediation and interpretation of Hedgehog signaling (Aza-Blanc *et al.*, 2000; Ruiz i Altaba, 1999). In mice, three GLI transcription factors (GLI1, GLI2, and GLI3) may possess distinct yet overlapping functions in Hh signaling, as determined by mutant analysis studies. A mutation in the human *Gli3* gene is responsible for Greig cephalopolysyn-

[1] To whom correspondence should be addressed. Fax: +81-48-467-6792. E-mail: jun@brain.riken.go.jp.

0012-1606/02 $35.00

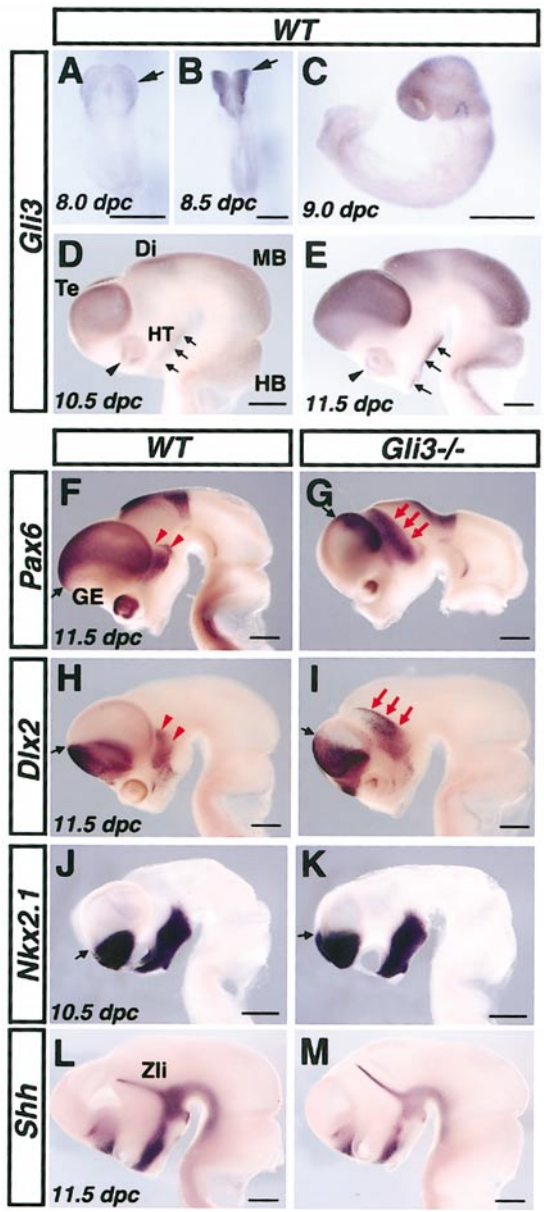

FIG. 1. Expanded ganglionic eminence and prosomere 3 (P3) region in *Gli3*$^{-/-}$ embryos. (A–E) Expression of *Gli3* mRNA in wild type embryos. (A, B) 8.0 and 8.5 dpc embryos, viewed from the dorsal surface. *Gli3* is expressed in the dorsal side of the head fold and neural crest region (arrow in A, B). (C) After neural tube closure, *Gli3* is expressed in the dorsal neural tube, strongly in the head (9.0 dpc embryo viewed from the lateral surface). (D–M) Brain at 10.5 and 11.5 dpc; mesenchymal cells and surface ectoderm have been removed; rostral is to the left. (D, E) *Gli3* mRNA is detected in the eye (arrowhead), hypothalamus (HT; arrows), dorsal telencephalon (Te), diencephalon (Di), midbrain (MB), and hindbrain (HB). (F, G) *Pax6* mRNA distribution in the wild type (F) and *Gli3*$^{-/-}$ (G) brain at 11.5 dpc. (F) *Pax6* is expressed in the dorsal telencephalon (black arrow), P3 region (ventral thalamus; red arrowheads), and dorsal part of P1 region (pretectum) of the diencephalon. (G) In *Gli3*$^{-/-}$ embryos, *Pax6* expression in the dorsal telencephalon is shifted toward the dorsal side (black arrow indicates the ventral edge of *Pax6* expression). *Pax6* expression in the P3 region is also expanded (red arrows in G). (H, I) *Dlx2* expression in the wild type (H) and *Gli3*$^{-/-}$ (I) embryo at 11.5 dpc. *Dlx2* is detected in the ganglionic eminence (black arrow) and P3 region (red arrowheads) in the wild type. (I) In *Gli3* mutants, *Dlx2* is expanded toward the dorsal side in the ganglionic eminence (black arrow indicates the position of dorsal edge of *Dlx2* expression). *Dlx2* expression in P3 region is also expanded (red arrows). (K) Expression of *Nkx2.1* in the ganglionic eminence is expanded dorsally (black arrow), while no change is seen in the hypothalamus. (L, M) Expression of *Shh* mRNA in the ventral midline of wild type (L) and *Gli3*$^{-/-}$ (M) brains at 11.5 dpc from the lateral view. (M) *Shh* (a ventral marker) is not affected in the ventral midline in *Gli3* mutants. Zli, zona limitans intrathalamica. Scale bars, 0.5 mm in (A–M).

dactyly syndrome (GCPS), an autosomal dominant disorder causing mild mental retardation, hypertelorism, strabismus, and polysyndactyly. The mouse *Gli3*$^{-/-}$ mutant *extratoes* (*Xt*^{J}) shows severe excencephaly, hypertelorism, cleft palate, eye malformation, bone malformation, and polysyndactyly (Johnson, 1967), making it a good model for studying GCPS. In the brain, the dorsal telencephalon is missing, resulting in a severe reduction of the cortex, olfactory bulb, and hippocampus (Theil *et al.*, 1999; Tole *et al.*, 2000). Although no obvious defect has been detected in the *Gli3*$^{-/-}$ spinal cord, GLI3 appears to be a major repressor of the development of ventral cell types (Litingtung and Chiang, 2000). In the spinal cord of *Shh*$^{-/-}$ mutants, all ventral cell types are missing. In contrast, in *Gli3*$^{-/-}$;*Shh*$^{-/-}$ double mutants, motor neurons, V1, and V2 progenitors are able to develop, suggesting that SHH is only required for floor plate and V3 interneuron induction when GLI3 is missing. GLI3 therefore appears to be a major repressor of the development of motor neurons, V1, and V2 progenitors in wild type mice.

In the limb bud, a mechanism underlying the *Gli3*$^{-/-}$ mutant polydactyly phenotype involving SHH has been postulated. Normally, *Shh* is expressed in zone of polarizing activity (ZPA) to organize anterior–posterior patterning during limb development. In the *Gli3*$^{-/-}$ mutant limb bud, ectopic *Shh* expression is detected on the anterior side, opposite to the ZPA (Masuya *et al.*, 1995). This ectopic SHH is thought to induce the mirror image duplication of the limb in *Gli3*$^{-/-}$ embryos, suggesting that GLI3 normally acts as a suppressor of *Shh* expression in the anterior part of the limb bud (Masuya *et al.*, 1995). However, the other abnormalities observed in *Gli3*$^{-/-}$ mutants, such as the absence of the dorsal forebrain, excencephaly, eye dysplasia, hypertelorism, and syndactyly, cannot be explained by this mechanism, since no other ectopic and/or expanded *Shh* expression domains are detected in *Gli3*$^{-/-}$ mutants. Therefore, we hypothesize that GLI3 has functions required for organogenesis that are independent of SHH signaling. We chose to investigate the expression of *Fgf8* in the abnormal tissues of *Gli3*$^{-/-}$ mutants, since FGF8 is also critical for the

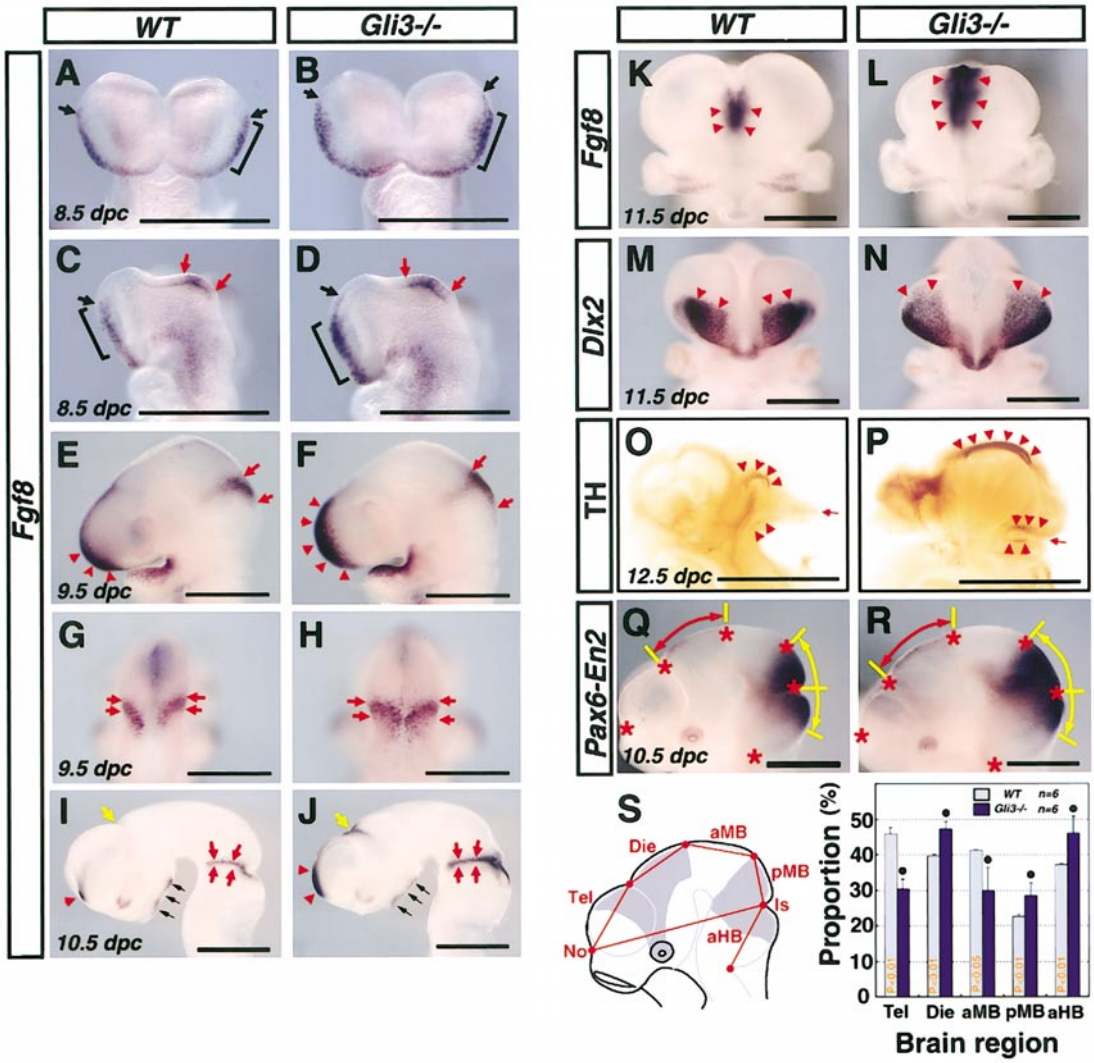

FIG. 2. Expansion of *Fgf8* expression in the *Gli3*$^{-/-}$ mutant brain. (A, C) *Fgf8* is expressed in the anterior neural ridge (sequence bracket) and isthmus (red arrows) at 8.5 dpc (A, frontal view; C, lateral view). (B, D) The *Fgf8* domain becomes wider in *Gli3*$^{-/-}$ mutants. Black arrow indicates the position of the posterior edge of *Fgf8* expression in the ANR in (A–D), and red arrows indicate anterior and posterior edge of *Fgf8* expression in the isthmus in (C–J). (E–H) After neural tube closure (9.5 dpc), *Fgf8* continues to be up-regulated in the ANR (red arrowheads) and isthmus (red arrows) in mutant embryos (E and F, lateral view; G and H, dorsal view). (I–N) Brain at 10.5 and 11.5 dpc after removal of mesenchymal cells and surface ectoderm. (I–L) All *Fgf8*-expression domains are expanded in the *Gli3*$^{-/-}$ mutant brain (ANR, red arrowheads; diencephalic region, yellow arrow; isthmus, red arrows) (I and J, lateral view; K and L, frontal view). *Dlx2* mRNA distribution in the wild type (M) and *Gli3*$^{-/-}$ brain (N) at 11.5 dpc, frontal view. (N) *Dlx2* expression is shifted dorsally in the mutant ganglionic eminence. (O, P) Tyrosine hydroxylase (TH) expression in wild type (O) and *Gli3*$^{-/-}$ (P) mutant brains at 12.5 dpc viewed from lateral side. TH-positive cells are detected in the diencephalon and around the isthmus (red arrowheads in O). The position of the isthmus is indicated by a red arrow. In the *Gli3*$^{-/-}$ brain, there is an increase in TH-positive neurons in the diencephalon and around the isthmus. (Q, R) *Pax6* and *En2* mRNA localization in wild type (Q) and *Gli3*$^{-/-}$ (R) mutant brains at 10.5 dpc for determination of changes in brain region size. Asterisks mark the boundary of each brain region for measurement (double-headed red arrow indicates diencephalic region defined by *Pax6* expression, double-headed yellow arrow indicates the isthmus marked by *En2* expression). (S) Schematic of brain regions measured. Graph of brain region proportions in wild type versus *Gli3*$^{-/-}$ mutants. There was a significant increase (*, $P < 0.05$) in size of the diencephalon (Die), posterior midbrain (pMB), and anterior hindbrain (aHB). There was a significant reduction (*, $P < 0.05$) in size of the telencephalon (Tel) and anterior midbrain (aMB). Scale bars, 1 mm in (A–N, Q, R); 5 mm in (O, P).

developmental patterning of the affected tissues. We found a marked up-regulation of *Fgf8* expression in the brain, eye, face, and limb buds in *Gli3*$^{-/-}$ mutants. We also found that programmed cell death was obviously reduced in these same *Fgf8*-expressing sites. Our observations suggest novel GLI3 functions in the control of *Fgf8* expression and apo-

ptosis in the developing neural tube, face, and limb, which is most likely independent of the SHH signaling cascade.

MATERIALS AND METHODS

Mice

Gli3$^{+/-}$ and *Shh*$^{+/-}$ mutant mice were obtained from The Jackson Laboratory (Bar Harbor, ME). *Gli3* mutant mice contain the *Xt*^{J}-specific fusion transcript generated by a deletion including all 3′ sequences of the *Gli3* locus. In *Shh* mutant mice, exon 2 is deleted by gene targeting (St-Jacques *et al.*, 1998). *Gli3*$^{+/-}$, *Shh*$^{+/-}$, and *Gli3*$^{+/-}$;*Shh*$^{+/-}$ mice were maintained in a mixed 129 and CD1 background. The generation and genotyping of mutant embryos were performed as described (Mo *et al.*, 1997; St-Jacques *et al.*, 1998, Maynard *et al.*, 2002). The stage of wild type and mutant embryos was determined by number of somite.

Whole-Mount in Situ Hybridization and Immunohistochemistry

Whole-mount *in situ* hybridization was performed as described (Motoyama *et al.*, 1998). The cDNA fragments were isolated by RT-PCR for use as templates in DIG-labeling *in vitro* transcription reactions, according to previous reports: *Dlx2* (Porteus *et al.*, 1991), *En2* (Millen *et al.*, 1994), *Fgf8* (Tanaka *et al.*, 1992), *Gli3* (Hui and Joyner, 1993), *Gremlin* (Lu *et al.*, 2001), *Nkx2.1* (Shimamura *et al.*, 1995), *Pax2* (Dressler *et al.*, 1990), *Pax6* (Walther and Gruss, 1991), *Pax7* (Mansouri *et al.*, 1996), *Pax9* (Neubüser *et al.*, 1995), and *Shh* (Echelard *et al.*, 1993). Embryos were photographed under a dissecting microscope.

The comparison of each brain region was done by measuring the distance between each region in brains on which *Pax6-En2* whole-mount *in situ* hybridization had been performed (10.5 dpc, $n = 6$ in each group). The proportion occupied by each brain region was determined as a percentage of the distance between the nose and the isthmus of the corresponding brain. Differences between wild type and *Gli3*$^{-/-}$ mutant brains were analyzed by Student's *t* test to determine the level of significance. The number of the *Fgf8*-expressing cells in the facial primordia and limb AER was determined by counting *Fgf8*-positive cells on photomicrographs of at least six wild type and *Gli3*$^{-/-}$ mutant embryos. Coronal and transverse sections were prepared for the facial primordia and AER, respectively. After *in situ* hybridization, four middle sections were chosen for counting, and the average per section was determined. Differences between wild type and *Gli3*$^{-/-}$ mutants were analyzed by Student's *t* test to determine the level of significance. To examine the phenotype of the neural tube and eye, some embryos were processed after removal of the facial epithelium and mesenchyme surrounding the neural tube. For *in situ* hybridization, we used *Gli3*$^{-/-}$ embryos without the excencephaly phenotype, since the morphology of the neural tube of exencephalic embryos is quite different from that of wild type. *Gli3*$^{-/-}$ embryos with normal neural tube closure comprised 40% of total homozygous embryos.

Immunodetection for tyrosine hydroxylase was done by using a rabbit anti-rat antibody (Chemicon International) as described (Ding *et al.*, 1998).

Apoptosis

Cell death was determined by TUNEL analysis. Wild type and mutant embryos were dissected at 8.5, 9.5, and 11.5 dpc and fixed with 4% paraformaldehyde in PBS. Whole-mount TUNEL reactions were performed according to the procedure provided (Intergen, Purchase, NY).

RESULTS

Brain Abnormalities in Gli3$^{-/-}$ *Mutants*

Gli3 was expressed in the dorsal edge of the neural plate in 8.0- to 8.5-dpc embryos (Figs. 1A and 1B). After neural tube closure, expression was restricted to the dorsal side of the neural tube, especially in the forebrain (Figs. 1C and 1D). In addition, *Gli3* was detected in the ventral forebrain within the hypothalamus, as well as in the eye from 10.5 dpc onwards (Figs. 1D and 1E).

Excencephaly or a reduced dorsal telencephalon has previously been reported in the *Gli3*$^{-/-}$ brain (Johnson, 1967; Theil *et al.*, 1999). We found similar defects in dorsal–ventral patterning in the *Gli3*$^{-/-}$ mutant brain. To define these defects, we performed marker gene analysis. In the wild type brain at 11.5 dpc, *Pax6* was expressed in the dorsal telencephalon, dorsal diencephalon (which includes prosomeres P1–P3), and optic cup (Fig. 1F). In *Gli3* $^{-/-}$ brains, *Pax6* expression in the telencephalon was greatly reduced, whereas expression in the P3 region of the diencephalon (ventral thalamus) was obviously expanded (Fig. 1G, black arrow and red arrows, respectively). No obvious difference in *Pax6* expression was observed in the P1 and P2 regions (dorsal hypothalamus) (Figs. 1F and 1G). Similar to previous reports, *Emx1* expression in the dorsal telencephalon was totally absent, while weak *Emx2* expression remained in the mutant brain (data not shown; Tole *et al.*, 2000). *Dlx2* localized in the ventral thalamus and ganglionic eminence in wild type brains (Fig. 1H). Expression was notably expanded in both the ventral thalamus, coinciding with the expansion of *Pax6* in this area (Figs. 1G and 1I, red arrows), and the ganglionic eminence in *Gli3*$^{-/-}$ mutants (Figs. 1H and 1I, black arrow). *Nkx2.1* was expressed in the ganglionic eminence and in the hypothalamus in the wild type brain (Fig. 1J). Consistent with *Dlx2* expression, *Nkx2.1* expression in the mutant ganglionic eminence was expanded dorsally (Fig. 1K, black arrow), whereas there was no difference in the hypothalamus (Figs. 1J and 1K). Together, these data reveal that, in addition to a reduced dorsal telencephalon, both the ganglionic eminence and P3 region of the diencephalon (ventral thalamus) were expanded dorsally in the *Gli3*$^{-/-}$ brain.

Shh is expressed in the basal plate of the telencephalon and zona limitans intrathalamica (Zli) in the wild type brain at 10.5 dpc (Fig. 1L). No expansion or ectopic *Shh* expression was observed in the *Gli3* mutant neural tube, indicating that the reduced dorsal telencephalon and expanded ganglionic eminence and dorsal hypothalamus are not caused by an expanded ventral structure (Figs. 1L and 1M). These observations led us to examine *Fgf8* expression in the mutant brain, since FGF8 in the anterior neural ridge is essential for the development of the ganglionic eminence

and also for the repression of the dorsal telencephalon (Crossley *et al.*, 2001).

Fgf8 Is Up-Regulated in the Gli3$^{-/-}$ Mutant Brain

In the developing wild type neural tube, *Fgf8* is expressed in the anterior neural ridge and isthmus (Figs. 2A, 2C, 2E, 2G, 2I, and 2K). Interestingly, *Fgf8* was up-regulated in the anterior neural ridge in *Gli3*$^{-/-}$ embryos at 8.5 dpc (Figs. 2B and 2D). The expansion of *Fgf8* became more obvious at later stages (Figs. 2F, 2H, 2J, and 2L). The increase in size of the mutant ganglionic eminence, determined by *Dlx2* and *Nkx2.1 in situ* analysis (Figs. 2M and 2N and Figs. 1J and 1K), correlated with the up-regulation of *Fgf8* expression, suggesting that FGF8 might induce the expansion of the ganglionic eminence (Figs. 2K–2N). *Fgf8* expression was also up-regulated in the isthmus (Figs. 2D, 2F, 2H, and 2J, red arrows). Furthermore, we observed more tyrosine hydroxylase-positive cells, presumptive dopaminergic neurons, in the forebrain and around the isthmus in *Gli3*$^{-/-}$ mutants (Figs. 2O and 2P). These neurons are induced by the combination of FGF8 and SHH in the forebrain and midbrain (Ye *et al.*, 1998), suggesting that the up-regulation of FGF8 can induce tyrosine hydroxylase-positive neuron differentiation in *Gli3*$^{-/-}$ mutants. We next analyzed *En2* expression to determine whether the boundary of the mutant isthmus was indeed expanded. Consistent with *Fgf8* expression, *En2* was also slightly expanded in the isthmus of the *Gli3*$^{-/-}$ brain (Figs. 2Q and 2R, yellow arrows). Thus, in addition to an expanded anterior neural ridge, we also found expansion of the isthmus in the *Gli3*$^{-/-}$ brain.

Using the expression patterns of *Pax6* and *En2*, we compared the relative size of each brain segment between wild type and *Gli3*$^{-/-}$ mutants (Fig. 2S). From this analysis, we found that the P3 region of the diencephalon (ventral thalamus), posterior midbrain, and anterior hindbrain was significantly expanded, while the dorsal telencephalon and anterior midbrain were reduced in size (Fig. 2S). These results indicate that not only dorsal–ventral patterning but also anterior–posterior patterning of the brain is affected in *Gli3*$^{-/-}$ embryos. Since FGF8 is essential for patterning the anterior neural ridge and isthmus, FGF8 up-regulation may be responsible for the alterations of these areas in the *Gli3*$^{-/-}$ brain.

Gli3 Is Required to Limit Optic Stalk Identity

We next examined how eye development is affected in *Gli3*$^{-/-}$ mutants, since *Gli3* is also expressed in the stalk region of the optic field (Figs. 3A and 3B). Interestingly, *Pax6* expression in the optic cup was greatly reduced in *Gli3*$^{-/-}$ mutants, whereas *Pax2* expression in the stalk was up-regulated (Figs. 3C–3F). The mutant optic stalk also became thicker than the wild type (Figs. 3E and 3F). Consistently, *Otx2* expression in the ventral half of the optic cup was reduced, whereas *Vax1* and *Vax2* expression in the optic stalk was expanded in the mutants (data not shown). This marker gene analysis indicates that more stalk cells and fewer optic cup cells comprise the optic field in *Gli3*$^{-/-}$ mutants, suggesting that GLI3 is needed to repress stalk identity in the optic field (Figs. 3G and 3H). Interestingly, we also observed an expansion of *Fgf8* expression in the optic stalk (Figs. 3I and 3J). It is possible that the expansion of the FGF8 domain impinges on the development of the optic cup.

Fgf8 Expression Is Up-Regulated in the Gli3$^{-/-}$ Mutant Face

Since we observed expanded *Fgf8* domains in all regions of the mutant neural tube, we hypothesized that *Fgf8* expression in other tissues may also be up-regulated to contribute to the malformations of *Gli3*$^{-/-}$ mutants. *Fgf8* expression in the facial primordia is important to maintain proliferation of mesenchymal cells (Figs. 4A and 4C) (Trumpp *et al.*, 1999). In *Gli3*$^{-/-}$ embryos, *Fgf8* expression was expanded in the facial primordia (Figs. 4B and 4D). We characterized the facial phenotype by analyzing *Pax9*, *Pax7*, and *Dlx2* expressions at 10.5 dpc. *Pax9* expression in the medial nasal process was obviously expanded in the mutants (Figs. 4E and 4F), which is consistent with the hypertelorism phenotype of GCPS patients. On the contrary, mesenchymal cells in the lateral nasal process marked by *Pax7* expression were reduced in the mutants (Figs. 4G and 4H). *Dlx2* is normally expressed in areas of the maxillary and mandibular processes (Fig. 4I). In *Gli3*$^{-/-}$ mutants, *Dlx2* delineated an expanded maxillary process, while the size of the mandibular process was not affected (Figs. 4I and 4J). Together, these data reveal an increase in mesenchymal cell number in the medial nasal process and maxillary process and a reduction in number in the lateral nasal process in *Gli3*$^{-/-}$ embryos. These data do not completely support a role for FGF8 in the expansion of facial domains, since the lateral nasal process is smaller in *Gli3*$^{-/-}$ mutants despite the up-regulation of *Fgf8* in this area. The mechanisms underlying this phenomenon require further investigation.

Fgf8 Is Up-Regulated in the Gli3$^{-/-}$ Mutant AER

Consistent with the brain, eye, and face, we also found that *Fgf8* expression in the apical ectodermal ridge (AER) of limb buds is up-regulated, by approximately twofold (Figs. 4K–4O). Many mice with mutations that result in the up-regulation of *Fgf8* in the AER show a syndactyly phenotype caused by the reduction of apoptosis in the interdigital regions (Jiang *et al.*, 1998). We therefore examined whether a decrease in apoptosis in *Gli3*$^{-/-}$ mutants may also underlie their syndactyly phenotype. Because we found that most *Fgf8*-expressing areas of the mouse embryo were abnormally expanded in *Gli3*$^{-/-}$ mutants, we evaluated both cell proliferation and apoptosis in these areas to ascertain the means by which these cell populations increased.

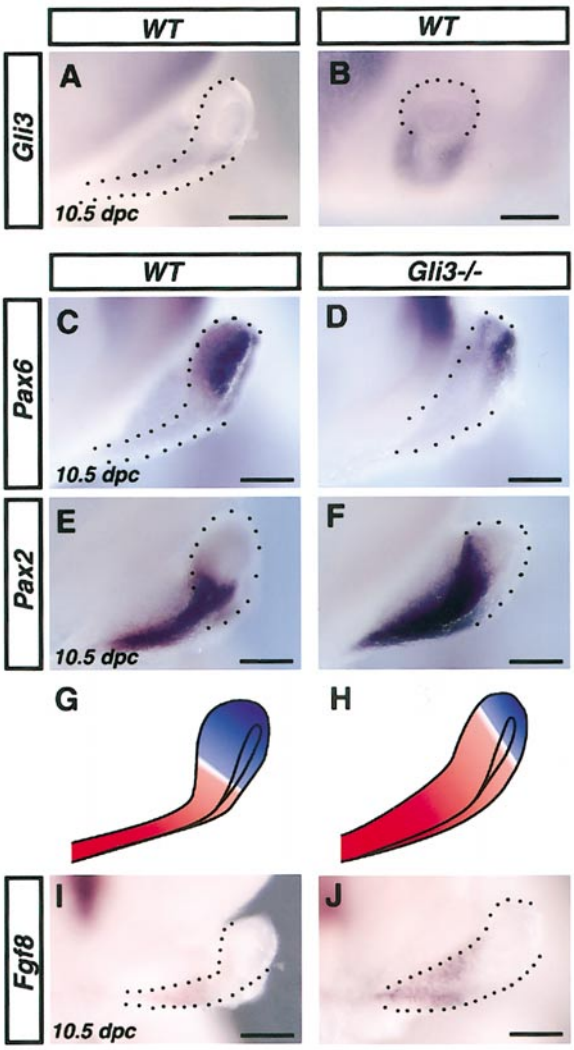

FIG. 3. Gli3$^{-/-}$ mutant mice have expanded optic stalk and reduced optic cup regions. (A, B) *Gli3* is expressed in the optic stalk (A, frontal view; B, lateral view) at 10.5 dpc. (C–F) Expression of the optic cup marker *Pax6* (C, D) and the optic stalk marker *Pax2* (E, F). (D) Expression of *Pax6* is reduced in the *Gli3*$^{-/-}$ mutant, whereas *Pax2* is expanded into the optic cup region in *Gli3*$^{-/-}$ embryos (F). (G, H) Schematic illustrations of the boundary between the optic stalk (red) and the optic cup (blue) in wild type (G) and *Gli3*$^{-/-}$ mutant (H) embryos. (I) *Fgf8* is expressed in optic stalk at 10.5 dpc, and expression is expanded in the *Gli3*$^{-/-}$ mutant (J). Scale bars, 1 mm.

Apoptosis Is Reduced in Gli3$^{-/-}$ Mutants

By BrdU labeling, we did not see any difference in cell proliferation between *Gli3*$^{-/-}$ mutants and wild type embryos in any areas (data not shown). Therefore, we examined cell death by TUNEL analysis. In the wild type mouse, many TUNEL-positive cells were detected in the anterior neural ridge, roof plate of the telencephalon, isthmus, facial primordia, and limb buds (Figs. 5A, 5C, 5E, and 5G). Interestingly, there was a consistent reduction of TUNEL-positive cells in *Gli3*$^{-/-}$ mutants (Figs. 5B, 5D, 5F, and 5H). In the mutant neural tube, apoptosis was reduced in the isthmus (Fig. 5B), anterior neural ridge, and roof plate (Fig. 5D), where we observed increased *Fgf8* expression, suggesting that the total number of the *Fgf8*-expressing cells is normally restricted by cell death.

Consistently, reduction of apoptosis was also detected in mutant limb buds at 9.5 and 11.5 dpc. In the wild type limb, we observed a mass of apoptosis in the AER and anterior necrotic area (Figs. 5E and 5G). In the *Gli3*$^{-/-}$ mutant limb, apoptosis in the AER was slightly reduced at 9.5 dpc (Fig. 5F). At 11.5 dpc, apoptosis was present in the AER similar to wild type, but there was no detectable apoptosis in the anterior necrotic area (Fig. 5H, black arrowheads). These data suggest that GLI3 is normally involved in the induction or maintenance of developmental cell death to limit the number of cells expressing *Fgf8*.

GLI3 Represses Fgf8 Expression Independently of SHH Signaling

The up-regulation of the *Fgf8* expression in the anterior neural ridge, isthmus, eye, facial primordia, and AER in *Gli3*$^{-/-}$ mutants (Figs. 6E, 6J, and 6Y) suggests that GLI3 normally functions to repress *Fgf8*. The balance between the activities of GLI3 and SHH may regulate *Fgf8* expression. To test this idea, we compared *Fgf8* expression patterns between *Gli3*$^{-/-}$, *Shh*$^{-/-}$, and *Gli3*$^{-/-}$;*Shh*$^{-/-}$ mutant embryos at 10.5 dpc. This approach is similar to Litingtung and Chiang (2000), in which they elucidated that GLI3 is a major repressor of motorneuron, V1, and V2 interneuron development. In our case, if GLI3 were a repressor of *Fgf8*, we would expect any loss of *Fgf8* in *Shh*$^{-/-}$ mutant mice to be rescued by the additional *Gli3* null mutation of *Gli3*$^{-/-}$; *Shh*$^{-/-}$ mice. First, we checked *Fgf8* expression in *Shh*$^{-/-}$ embryos. *Shh*$^{-/-}$ embryos showed severe holoprocencephaly, and *Fgf8* levels were notably reduced in the anterior neural ridge, isthmus, and AER, while expression in the facial primordia was not affected (Figs. 6B, 6G, and 6V). Interestingly, in *Gli3*$^{-/-}$;*Shh*$^{-/-}$ double mutants, *Fgf8* was up-regulated in the neural tube, facial primordia, and AER, similar to levels in *Gli3*$^{-/-}$ mutants (Figs. 6D, 6E, 6I, 6J, 6X, and 6Y). These observations suggest that SHH is not required for either the activation or maintenance of *Fgf8* when GLI3 is also absent. Thus, GLI3 indeed functions as a repressor of *Fgf8* expression independently of SHH signaling. The rescue of *Fgf8* levels by the addition of a *Gli3* null mutation in the *Shh*$^{-/-}$ background occurs in a gene dose-dependent manner. We found slightly more *Fgf8* expression in the anterior neural ridge, isthmus, and AER of *Gli3*$^{+/-}$; *Shh*$^{-/-}$ embryos compared with those in *Shh*$^{-/-}$ mutants (Figs. 6C, 6H, and 6W).

GLI3 is expressed in the dorsal half of the telencephalon (Fig. 6K). Interestingly, *Gli3* expression was obviously ex-

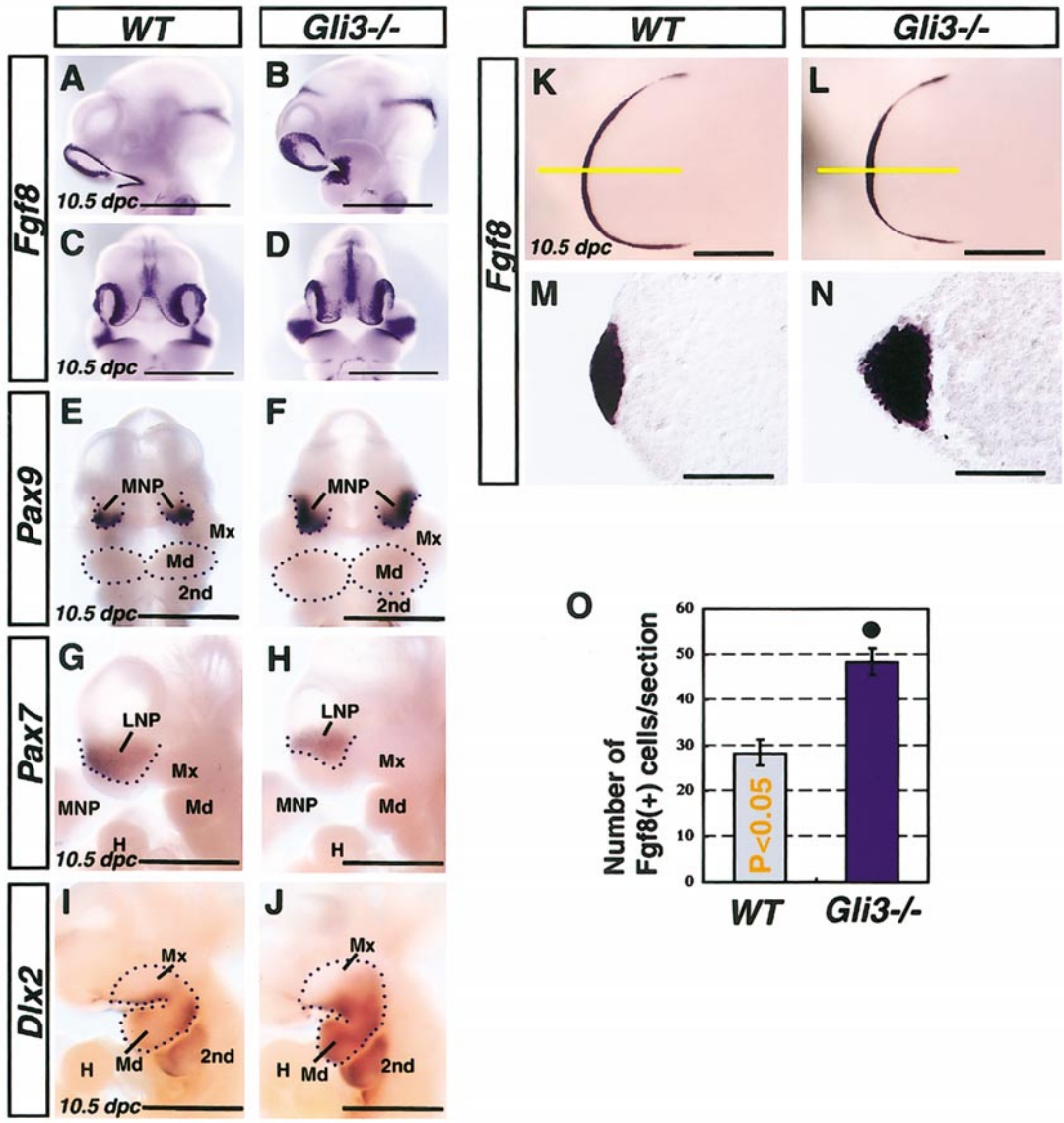

FIG. 4. Expansion of *Fgf8* gene expression in the face and limb bud in *Gli3*$^{-/-}$ mutants. Expression of *Fgf8* mRNA in wild type (A, C) and *Gli3*$^{-/-}$ mutants (B, D) viewed from lateral view (A, B) and frontal view (C, D) at 10.5 dpc. *Fgf8* is expressed in the epithelium of the facial primordium. (B, D) *Fgf8* expression in all facial primordia is expanded. (E and F, frontal view) *Pax9* is expressed in the medial nasal process (MNP), which is expanded in the mutant face (F). (G and H, lateral view) *Pax7* is expressed in lateral nasal process (LNP), which is reduced in the mutant face (H). (I and J, lateral view) *Dlx2* is detected in the maxillary and mandibular processes (Mx, Md), which are expanded in the mutant face. *Fgf8* mRNA distribution in the AER of wild type (K, M) and *Gli3*$^{-/-}$ (L, N) limb bud at 10.5 dpc. (M, N) Transverse section at yellow line of (K) and (L). (O) The number of *Fgf8*-positive cells in the AER of *Gli3*$^{-/-}$ embryos is significantly increased (*, $P < 0.05$) compared with wild type embryos. 2nd, second pharyngeal arch; H, heart primordium. Scale bars, 2 mm in (A–J); 0.5 mm in (K, L); 0.1 mm in (M, N).

panded toward the ventral side of the telencephalon in *Shh*$^{-/-}$ mutants (Figs. 6L and 6M). Consistently, *Pax6* expression marking the dorsal telencephalon was also shifted to the ventral side in *Shh*$^{-/-}$ mutants (Fig. 6Q), indicating that the brain is highly dorsalized. This expanded dorsal phenotype was rescued by the superimposed *Gli3* null mutation of *Gli3*$^{-/-}$;*Shh*$^{-/-}$ mice (Figs. 6R–6T), indicating that GLI3 normally has a dorsalizing role in wild type neural development.

As we have described, reduced apoptosis is observed in *Gli3*$^{-/-}$ mutants, while excessive cell death is observed in *Shh*$^{-/-}$ mutants (data not shown; Ohkubo *et al.*, 2002). It

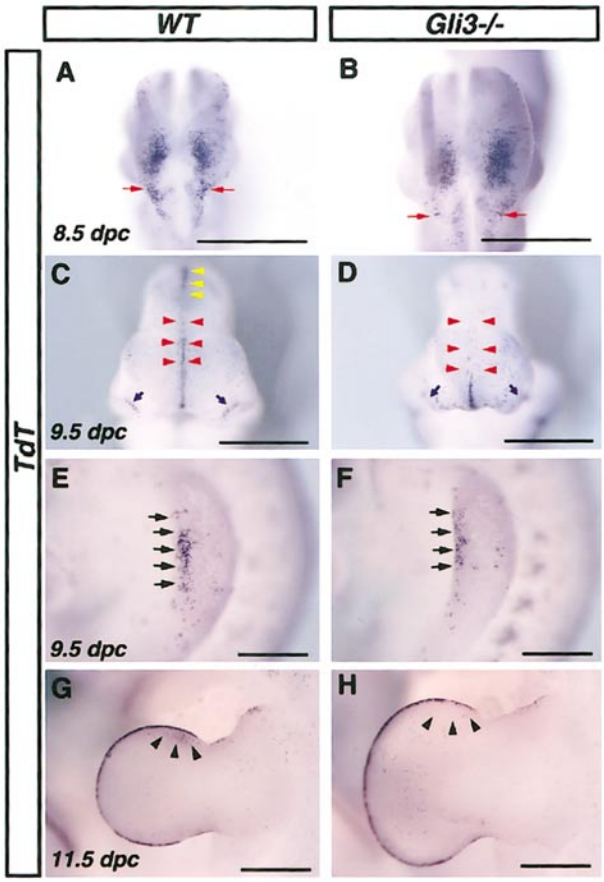

FIG. 5. Reduction of apoptosis in the isthmus, anterior neural ridge, and apical ectodermal ridge of *Gli3*$^{-/-}$ mutants. Whole-mount TUNEL analysis in wild type (A, C, E, G) and *Gli3*$^{-/-}$ embryos (B, D, F, H). (A) Cell death in the isthmus is detected at 8.5 dpc (dorsal view). (B) There are fewer TdT-positive cells in the isthmus of *Gli3*$^{-/-}$ mutants (red arrows). (C, D) Cell death in the anterior neural ridge (red arrowheads), dorsal midbrain region (yellow arrowheads), and nasal epithelium (blue arrows) is detected at 9.5 dpc, and is notably reduced in the mutant brain (frontal views). (E, F) Cell death in the apical ectodermal ridge (AER) of the limb bud is detected at 9.5 dpc in wild type embryos (lateral view). In *Gli3*$^{-/-}$ embryos, there are fewer TdT-positive cells (black arrows). (G, H) At 11.5 dpc, TdT is detected in the anterior necrotic area (black arrowheads) in addition to the AER. In *Gli3*$^{-/-}$ embryos, TdT is not detectable in the anterior necrotic area (black arrowheads), though there is no difference in the AER. Scale bars, 1 mm in (A–H).

has been postulated that the excessive cell death in *Shh*$^{-/-}$ mutants may result from the activation of BMP signaling (Ohkubo *et al.*, 2002). One mechanism by which BMP signaling can be activated is by a reduction of GREMLIN, an antagonist of BMP signaling, so we performed *in situ* hybridization to compare *Gremlin* mRNA localization and intensity between wild type and *Gli3*$^{-/-}$ mutant mice. In the wild type, *Gremlin* localized to the posterior half of the limb buds, the juncture of the maxillary and mandibular processes, and in somites (data not shown). A difference in *Gremlin* expression was detected in the *Gli3*$^{-/-}$ limb bud, where it was expressed in the entire progress zone (Figs. 6e and 6i). Figs. 6U–6i show the relationship between *Shh*, *Gli3*, *Fgf8*, and *Gremlin* in the developing limb bud. In *Shh*$^{-/-}$ mutants, *Gremlin* expression was completely absent in the limb bud (Fig. 6f), which may permit an increase in apoptosis via BMP signaling and thus decrease the number of *Fgf8*-expressing cells (Fig. 6V). In the double mutant (*Gli3*$^{-/-}$;*Shh*$^{-/-}$), *Gremlin* is detectable throughout the entire progress zone, indicating that GLI3 is normally an important repressor of *Gremlin* expression (Fig. 6h). This idea is further supported by the localization of *Gli3* itself in the limb bud of each mouse. Compared with the wild type limb, where *Gli3* expression is restricted to the anterior portion (Fig. 6Z), in *Shh*$^{-/-}$ mice, *Gli3* is expressed throughout (Fig. 6a) and could thus inhibit *Gremlin* transcription in the posterior area as well. The lack of *Gli3* in the *Gli3*$^{-/-}$ mutant limb bud (Figs. 6b–6d), conversely allows more *Gremlin* to be transcribed. The up-regulation of *Gremlin* could then inhibit apoptosis by decreasing BMP signaling, resulting in the increase in *Fgf8*-expressing cells in the AER (Figs. 6W–6Y). The lower level of *Gremlin* expression in *Gli3*$^{-/-}$;*Shh*$^{-/-}$ double mutants compared with *Gli3*$^{-/-}$ mutants (Figs. 6h and 6i) suggests that SHH may normally be involved in the transcriptional activation of *Gremlin*.

DISCUSSION

In this study, we provide evidence that GLI3 is involved in the suppression of *Fgf8* in the developing mouse embryo. The up-regulation of *Fgf8* expression in *Gli3*$^{-/-}$ mutants may be sufficient to explain their developmental abnormalities, which can be extended to explain the abnormalities of human GCPS. Since FGF8 is essential for the control of pattern formation in many sites of the embryo, the up-regulation of *Fgf8* can affect the developmental programs of many tissues. Our results also suggest that GLI3 promotes developmental apoptosis in the anterior neural ridge, isthmus, facial primordia, and AER. Herein, we discuss the implications of these findings with references.

The Up-Regulation of Fgf8 and Gli3$^{-/-}$ *Neural Abnormalities*

In this study, we found expansion of the ganglionic eminence, P3 region of the diencephalon (ventral thalamus), and isthmus in the *Gli3*$^{-/-}$ mutant brain, and a reduction of the dorsal telencephalon (Fig. 2S) (Johnson, 1967; Theil *et al.*, 1999; Tole *et al.*, 2000). The up-regulation of FGF8 in the anterior neural ridge might explain the expansion of the ganglionic eminence and reduction of dorsal telencephalon in *Gli3*$^{-/-}$ brain, since FGF8 is thought to have dual activities in this region: one to induce the ganglionic eminence and the other to suppress the character

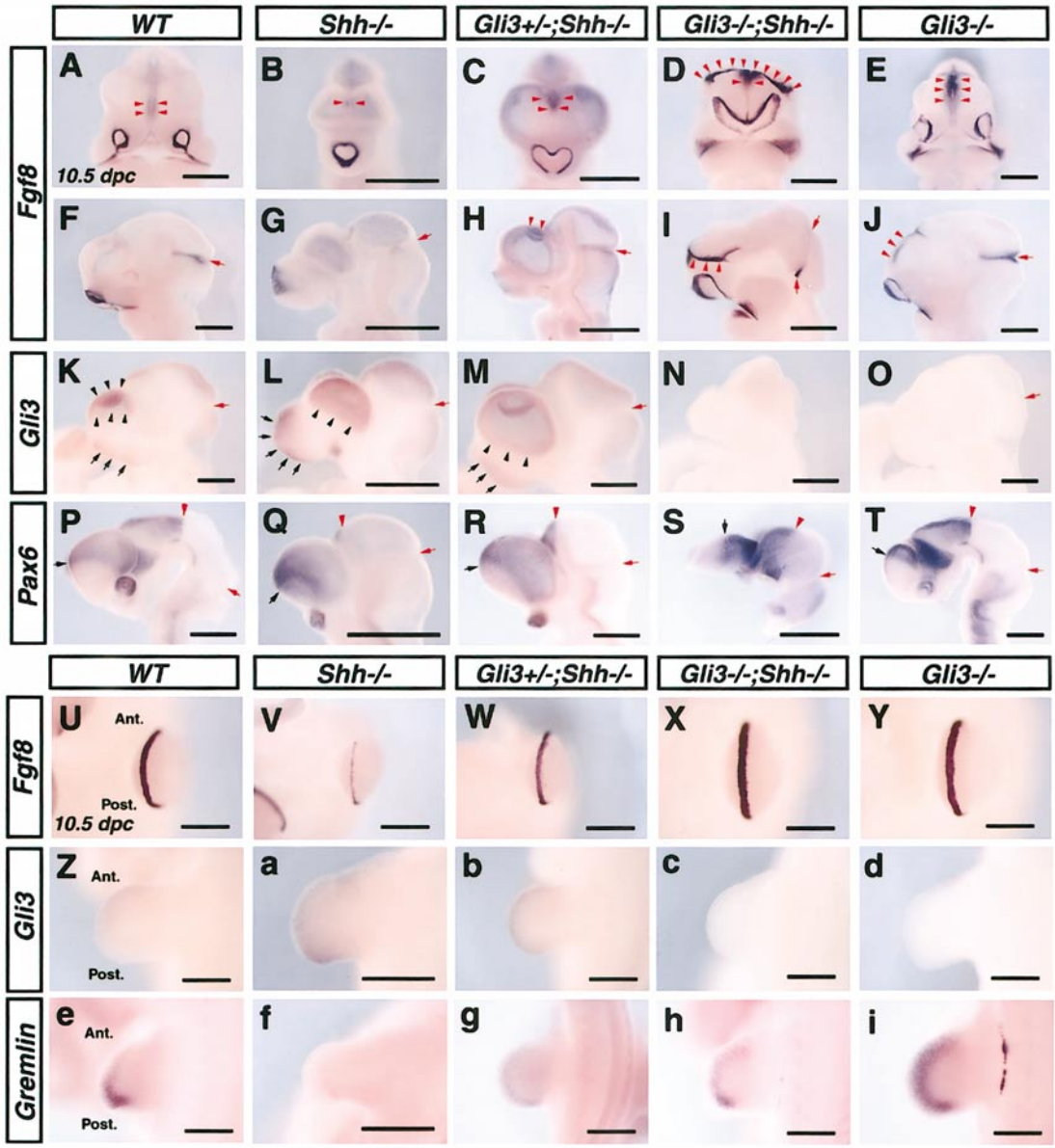

FIG. 6. SHH is not involved in the regulation of *Fgf8* expression by GLI3. (A–J) Expression of *Fgf8* mRNA in the ANR (red arrowheads), isthmus (red arrow), and face. Frontal (A–E) and lateral views (F–J) of 10.5-dpc embryos. In the ANR and isthmus of $Shh^{-/-}$ mutants, *Fgf8* is very weakly expressed (B, G). *Fgf8* expression is recovered in the ANR and isthmus of $Gli3^{+/-}$;$Shh^{-/-}$ (C, H) and $Gli3^{-/-}$;$Shh^{-/-}$ mutants (D, I). (K–O) *Gli3* mRNA is detected in dorsal telencephalon and facial primordia of WT embryos (K, lateral view). In $Shh^{-/-}$ and $Gli3^{+/-}$;$Shh^{-/-}$ mutants, *Gli3* expression is expanded ventrally in the telencephalon (L, M). Black arrowheads indicate the ventral edge of *Gli3* expression in the telencephalon. *Gli3* in the nasal process is also expanded in these mutants (black arrows). In $Gli3^{-/-}$;$Shh^{-/-}$ and $Gli3^{-/-}$ embryos, *Gli3* expression is not detected (N, O). (P–T) *Pax6* mRNA is detected in the dorsal telencephalon and diencephalon of wild type brains (P). Black arrow and red arrowhead show the ganglionic eminence–cortex boundary and diencephalon–midbrain boundary, respectively. Red arrow shows the isthmus. (Q) *Pax6* is expressed more ventrally in $Shh^{-/-}$ mutants. (R, S) The ganglionic eminence structure is recovered in $Gli3^{+/-}$;$Shh^{-/-}$ and $Gli3^{-/-}$;$Shh^{-/-}$ embryos. (U–Y) *Fgf8* expression in the AER, apical view. (V) In $Shh^{-/-}$ mutants, *Fgf8* is very weakly expressed. (W, X) The expression of *Fgf8* is recovered in $Gli3^{+/-}$;$Shh^{-/-}$ and $Gli3^{-/-}$;$Shh^{-/-}$ embryos. Note that the expansion of *Fgf8* in the AER of $Gli3^{-/-}$;$Shh^{-/-}$ embryos (X) is similar to that in $Gli3^{-/-}$ embryos (Y). (Z) *Gli3* mRNA is detected in the anterior portion of the limb bud. (a, b) *Gli3* is expanded into the posterior portion in $Shh^{-/-}$ and $Gli3^{+/-}$;$Shh^{-/-}$ embryos. (c, d) No *Gli3* expression is detected in $Gli3^{-/-}$;$Shh^{-/-}$ and $Gli3^{-/-}$ mutants. (e) *Gremlin* expression is detected in the posterior portion of the wild type limb bud. (f) In $Shh^{-/-}$ mutants, *Gremlin* is very weakly expressed. (g, h) *Gremlin* expression is recovered in $Gli3^{+/-}$;$Shh^{-/-}$ and $Gli3^{-/-}$;$Shh^{-/-}$ double mutants, and is also detectable on the anterior side. (i) In $Gli3^{-/-}$ mutants, expression of *Gremlin* is strongly expanded into the anterior portion. Limb buds in (U–i) are forelimb buds with anterior (Ant.) at the top and posterior (Post.) at the bottom. Scale bars, 1 mm in (A–T); 0.5 mm in (U–i).

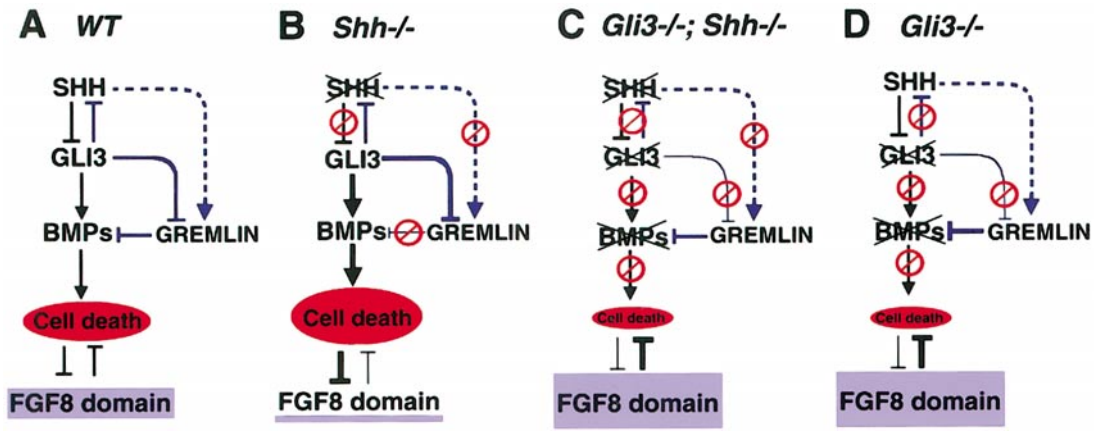

FIG. 7. GLI3 regulates cell death and the size of FGF8 domains. (A) In wild type embryos, SHH inhibits *Gli3* gene expression in many sites. Where GLI3 is present, it activates the expression of *Bmps*, which regulates cell death to alter the size of FGF8 domains. In the limb bud only (blue lines), GLI3 also represses the BMP antagonist *Gremlin*. (B) In $Shh^{-/-}$ embryos, GLI3 has more effect in up-regulating *Bmp* and inhibiting *Gremlin* expressions, which leads to an increase in cell death. As a result, FGF8 domains are reduced. (C) In $Gli3^{-/-};Shh^{-/-}$ embryos, *Bmps* are reduced and *Gremlin* is more widely expressed in the limb bud, contributing to a decrease in cell death and hence an increase in number of FGF8-expressing cells. (D) In $Gli3^{-/-}$ embryos, the outcome is similar to $Gli3^{-/-};Shh^{-/-}$ embryos; a reduction of cell death leads to the expansion of FGF8 domains. Therefore, the regulation of FGF8 domain size by *Gli3* is independent of SHH function. The blue pathway is only observed in limb buds.

of the dorsal forebrain (Crossley *et al.*, 2001). The enlargement of the ventral thalamus in $Gli3^{-/-}$ mice might be explained by a different mechanism, since *Fgf8* is not expressed in the ventral diencephalon, but this remains to be determined. *Bmps*, *Wnt1*, *Wnt3a*, and *Wnt8b* are all reduced in $Gli3^{-/-}$ mutant brains (Tole *et al.*, 2000, Theil *et al.*, 2002; data not shown), and are thus candidates for the regulation of thalamus development. We know from our data that GLI3 must normally suppress the development of the ventral thalamus (through induction of BMPs or Wnts perhaps), since in $Gli3^{-/-};Shh^{-/-}$ double mutants the ventral thalamus is able to develop, whereas in $Shh^{-/-}$ single mutants the ventral thalamus is completely missing (Figs. 6Q–6S).

The isthmus is also expanded in the $Gli3^{-/-}$ mutant brain. An expanded *Fgf8* domain is likely responsible for the expansion of the isthmus, since FGF8 is known to induce the isthmus-restricted transcription factor *En2* (Sato *et al.*, 2001). The expansion of the isthmus may cause the concomitant enlargement of the posterior midbrain and anterior hindbrain, since both of these brain segments face the isthmus and may thus receive heightened FGF8 signals. Furthermore, tyrosine hydroxylase (TH)-positive cells, which are induced by FGF8 and SHH (Ye *et al.*, 1998), are more numerous around the mutant forebrain and isthmus, demonstrating greater FGF8 signaling in the forebrain and peri-isthmus region in $Gli3^{-/-}$ mutants.

In the developing eye, both *Gli3* and *Fgf8* are expressed in the optic stalk. In $Gli3^{-/-}$ embryos, the stalk is expanded, while the optic cup is reduced (Fig. 3). It has been shown that the administration of exogenous FGF8 can induce an increase in optic stalk and reduction in optic cup identity if it is applied prior to the invagination of the optic field (Crossley *et al.*, 2001). We found an up-regulation of *Fgf8* in the anterior neural ridge at 8.5 dpc, before invagination of the optic field, suggesting that the increase in FGF8 results in the expansion of the presumptive stalk region.

Abnormal Brain and Face Development in Gli3 Mutants

Similar to human GCPS patients, the medial nasal process and maxillary process are enlarged in $Gli3^{-/-}$ mutants, whereas the lateral nasal process is reduced. An increase in FGF8 cannot explain these changes, since *Fgf8* expression patterns do not completely correlate with these facial changes (Fig. 4). It is possible that abnormal brain development may instead be the cue for these facial malformations. Mesenchymal cells in the facial primordia are derived from the migration of cranial neural crest cells from particular brain segments (Noden, 1983; Couly *et al.*, 1998). Most of the cells in the medial nasal process are derived from the forebrain, whereas the lateral nasal process is derived from the anterior midbrain. The cells in the maxillary process originate in the posterior midbrain, while the mandibular process is derived from both posterior midbrain and anterior hindbrain. The abnormal proportions of the $Gli3^{-/-}$ mutant brain may thus affect the number of neural crest cells migrating to the facial primordia: more cells from expanded segments (diencephalon and posterior midbrain) to the medial nasal process and maxillary process, and fewer cells

from the reduced segment (anterior midbrain) to the lateral nasal process.

The Relationship between GLI3, BMP Signaling, Apoptosis, and FGF8

Our investigations of *Fgf8* expression in *Gli3*$^{-/-}$ mice revealed a ubiquitous up-regulation of *Fgf8* in all areas where developmental malformations are observed. However, we did not detect any difference in *Fgf8* expression in areas that are not affected in *Gli3*$^{-/-}$ mice, namely the hypothalamus, somites, and the pharyngeal endoderm. We ascertained that there was a general increase in the number of *Fgf8*-expressing cells in areas with expanded *Fgf8* domains. The question then was how the lack of *Gli3* could ultimately result in an increase in *Fgf8*-expressing cell number. We investigated both cell proliferation and apoptosis to determine how *Fgf8*-expressing cells increased in number in *Gli3*$^{-/-}$ mutants and found a decrease in apoptosis in areas coinciding with expanded FGF8 domains.

The mechanism by which GLI3 can increase apoptosis is not currently known, but our data and others support a role for BMP signaling in this phenomenon, wherein BMP signaling can increase apoptosis in some tissues. An endogenous inhibitor of BMP signaling, GREMLIN, has therefore also been implicated in the regulation of apoptosis. Treatment of chick limb buds with GREMLIN protein causes the expansion of the AER, reduction of apoptosis, and enlargement of the limb bud without any obvious modifications of *Bmp* expression (Merino *et al.*, 1999). In *Gli3*$^{-/-}$ mutant limb buds, we found that *Gremlin* expression was ectopically expressed throughout the limb bud, whereas in the wild type, it is restricted to the posterior side (Fig. 6). On the contrary, no obvious difference in *Bmps* expression in the *Gli3*$^{-/-}$ mutant limb bud has been reported (Buscher *et al.*, 1997). In the wild type, therefore, GLI3 must inhibit *Gremlin* expression in the anterior limb bud, the only location where GLI3 is expressed. In the *Gli3*$^{-/-}$ mutant limb bud, *Gremlin* is relieved from inhibition and expressed ubiquitously, which may lead to a decrease in BMP-induced apoptosis.

In *Gli3*$^{-/-}$ mutant brains, *Bmps* expression has previously been evaluated, and *Bmp2*, *Bmp4*, *Bmp6*, and *Bmp7* are all strikingly reduced by *in situ* hybridization analyses (Tole *et al.*, 2000). Local administration of exogenous BMP4 in the forebrain at the neural plate stage increases cell death and reduces both *Fgf8* and *Shh* expressions (Furuta *et al.*, 1997; Ohkubo *et al.*, 2002). Since we did not detect any obvious reduction of BMP inhibitors in the *Gli3*$^{-/-}$ brain (data not shown), the reduction of cell death in the mutant brain may result from reduced *Bmp* expression. Thus, the reduction of BMP signaling in *Gli3*$^{-/-}$ mutants, either by the increase in *Gremlin* expression or by a decrease in *Bmp* expression, may be pivotal in the reduction of apoptosis throughout the mutant embryo.

The Role of SHH in the Regulation of Fgf8 Expression

We evaluated differences in *Fgf8* levels in *Shh*$^{-/-}$ mutants compared with *Gli3*$^{-/-}$ and *Gli3*$^{-/-}$;*Shh*$^{-/-}$ double mutants at 10.5 dpc to determine whether SHH was playing a role in *Fgf8* regulation. In *Shh*$^{-/-}$ mutants, *Fgf8* expression was reduced in all expression domains, suggesting that SHH is required for *Fgf8* expression. If SHH is required for the development of the cells expressing *Fgf8*, we would expect no difference in *Fgf8* expression in *Shh*$^{-/-}$ single and *Gli3*$^{-/-}$;*Shh*$^{-/-}$ double mutants. However, these double mutants displayed an increase in *Fgf8* expression, similar to *Gli3*$^{-/-}$ mutants, indicating that loss-of-function of *Gli3* regulates *Fgf8* expression independently of SHH signaling. In the *Shh*$^{-/-}$ mutant limb bud, Chiang *et al.* (2001) have recently found that *Fgf8* is present in early gestation, but as the AER deteriorates so too does *Fgf8* expression decrease. Because *Gli3* is ubiquitously expressed in the *Shh*$^{-/-}$ limb bud, GLI3 might be contributing to the deterioration of the AER by increasing cell death. In support of this hypothesis, the excessive apoptosis in *Shh*$^{-/-}$ mutants disappears in *Gli3*$^{-/-}$;*Shh*$^{-/-}$ double mutants (Litingtung and Chiang, 2000).

In this study, we found a marked increase in *Gli3* expression in the *Shh*$^{-/-}$ brain, face, and limb buds, suggesting that SHH represses *Gli3* transcription in the wild type. This observation is consistent with their expression patterns, which are segregated from each other. The repression of *Gli3* by SHH might limit *Gli3* expression to the anterior half of the limb bud, in the same way that it limits *Gli3* to the dorsal side of the neural tube (Figs. 1 and 6). Our data are summarized in Fig. 7, in diagrams depicting the relationship between SHH, GLI3, BMP signaling, apoptosis, and the size of *Fgf8* domains in the different backgrounds analyzed in this study. In the wild type mouse (Fig. 7A), GLI3 may positively regulate BMP-induced cell death by the activation of *Bmp* expression or the suppression of *Gremlin* expression to limit the number of the cells expressing *Fgf8*. Thus, the balance between cell proliferation and cell death may be critical for the proper assignment of *Fgf8*-expressing cells in the developing neural tube, face, and limb buds. In *Shh*$^{-/-}$ mutant embryos (Fig. 7B), *Gli3* expression is expanded, resulting in more cell death and hence reduced FGF8 domains. The phenotype of *Gli3*$^{-/-}$;*Shh*$^{-/-}$ embryos is quite similar to that of *Gli3*$^{-/-}$ single mutants (Figs. 7C and 7D). Without GLI3, up-regulated *Fgf8* expression is not altered whether SHH is present or not, suggesting that SHH is not directly involved in the regulation of *Fgf8* expression by GLI3.

Although we still have many unanswered questions, our results suggest that GLI3 is essential for pattern formation in the developing brain, face, and limb. GLI3 may determine the size of *Fgf8*-expressing domains by the modification of cell death. Further analysis is required to determine how GLI3 modulates cell death through BMP signaling or other pathways.

ACKNOWLEDGMENTS

We thank Drs. Akihiko Koseki, Isao Matsuo, John Rubenstein, and Shingi Takada for providing probes for *in situ* hybridization. This work is supported by a Grant-in-Aid from the Ministry of Education, Culture, Sports, Science and Technology, Japan (to J.M.).

REFERENCES

Aza-Blanc, P., Lin, H. Y., Ruiz i Altaba, A., and Kornberg, T. B. (2000). Expression of the vertebrate Gli proteins in Drosophila reveals a distribution of activator and repressor activities. *Development* **127,** 4293–4301.

Buscher, D., Bosse, B., Heymer, J., and Rüther, U. (1997). Evidence for genetic control of Sonic hedgehog by Gli3 in mouse limb development. *Mech. Dev.* **62,** 175–182.

Chiang, C., Litingtung, Y., Lee, E., Young, K. E., Corden, J. L., Westphal, H., and Beachy, P. A. (1996). Cyclopia and defective axial patterning in mice lacking Sonic hedgehog gene function. *Nature* **383,** 407–413.

Chiang, C., Litingtung, Y., Harris, M. P., Simandl, B. K., Li, Y., Beachy, P. A., and Fallon, J. F. (2001). Manifestation of the limb prepattern: Limb development in the absence of sonic hedgehog function. *Dev. Biol.* **236,** 421–435.

Couly, G., Grapin-Botton, A., Coltey, P., Ruhin, B., and Le Douarin, N. M. (1998). Determination of the identity of the derivatives of the cephalic neural crest: Incompatibility between Hox gene expression and lower jaw development. *Development* **125,** 3445–3459.

Crossley, P. H., Martinez, S., Ohkubo, Y., and Rubenstein, J. L. (2001). Coordinate expression of Fgf8, Otx2, Bmp4, and Shh in the rostral prosencephalon during development of the telencephalic and optic vesicles. *Neuroscience* **108,** 183–206.

Ding, Q., Motoyama, J., Gasca, S., Mo, R., Sasaki, H., Rossant, J., and Hui, C. C. (1998). Diminished Sonic hedgehog signaling and lack of floor plate differentiation in Gli2 mutant mice. *Development* **125,** 2533–2543.

Dressler, G. R., Deutsch, U., Chowdhury, K., Nornes, H. O., and Gruss, P. (1990). Pax2, a new murine paired-box-containing gene and its expression in the developing excretory system. *Development* **109,** 787–795.

Echelard, Y., Epstein, D. J., St-Jacques, B., Shen, L., Mohler, J., McMahon, J. A., and McMahon, A. P. (1993). Sonic hedgehog, a member of a family of putative signaling molecules, is implicated in the regulation of CNS polarity. *Cell* **75,** 1417–1430.

Furuta, Y., Piston, D. W., and Hogan, B. L. (1997). Bone morphogenetic proteins (BMPs) as regulators of dorsal forebrain development. *Development* **124,** 2203–2212.

Hui, C. C., and Joyner, A. L. (1993). A mouse model of Greig cephalopolysyndactyly syndrome: The extra-toesJ mutation contains an intragenic deletion of the *Gli3* gene. *Nat. Genet.* **3,** 241–246.

Ingham, P. W. (1998). The patched gene in development and cancer. *Curr. Opin. Genet. Dev.* **8,** 88–94.

Ingham, P. W., and McMahon, A. P. (2001). Hedgehog signaling in animal development: paradigms and principles. *Genes Dev.* **15,** 3059–3087.

Jiang, R., Lan, Y., Chapman, H. D., Shawber, C., Norton, C. R., Serreze, D. V., Weinmaster, G., and Gridley, T. (1998). Defects in limb, craniofacial, and thymic development in Jagged2 mutant mice. *Genes Dev.* **12,** 1046–1057.

Johnson, D. R. (1967). Extra-toes: A new mutant gene causing multiple abnormalities in the mouse. *J. Embryol. Exp. Morphol.* **17,** 543–581.

Litingtung, Y., and Chiang, C. (2000). Specification of ventral neuron types is mediated by an antagonistic interaction between Shh and Gli3. *Nat. Neurosci.* **3,** 979–985.

Lu, M. M., Yang, H., Zhang, L., Shu, W., Blair, D. G., and Morrisey, E. E. (2001). The bone morphogenic protein antagonist gremlin regulates proximal-distal patterning of the lung. *Dev. Dyn.* **222,** 667–680.

Mansouri, A., Stoykova, A., Torres, M., and Gruss, P. (1996). Dysgenesis of cephalic neural crest derivatives in $Pax7^{-/-}$ mutant mice. *Development* **122,** 831–838.

Masuya, H., Sagai, T., Wakana, S., Moriwaki, K., and Shiroishi, T. (1995). A duplicated zone of polarizing activity in polydactylous mouse mutants. *Genes Dev.* **9,** 1645–1653.

Maynard, T. M., Jain, M. D., Balmer, C. W., and LaMantia, A. S. (2002). High-resolution mapping of the Gli3 mutation Extra-toesJ reveals a 51.5-kb deletion. *Mamm. Genome* **13,** 58–61.

Merino, R., Rodriguez-Leon, J., Macias, D., Ganan, Y., Economides, A. N., and Hurle, J. M. (1999). The BMP antagonist Gremlin regulates outgrowth, chondrogenesis and programmed cell death in the developing limb. *Development* **126,** 5515–5522.

Methot, N., and Basler, K. (2001). An absolute requirement for Cubitus interruptus in Hedgehog signaling. *Development* **128,** 733–742.

Millen, K. J., Wurst, W., Herrup, K., and Joyner, A. L. (1994). Abnormal embryonic cerebellar development and patterning of postnatal foliation in two mouse Engrailed-2 mutants. *Development* **120,** 695–706.

Mo, R., Freer, A. M., Zinyk, D. L., Crackower, M. A., Michaud, J., Heng, H. H., Chik, K. W., Shi, X. M., Tsui, L. C., Cheng, S. H., Joyner, A. L., and Hui, C. (1997). Specific and redundant functions of Gli2 and Gli3 zinc finger genes in skeletal patterning and development. *Development* **124,** 113–123.

Motoyama, J., Liu, J., Mo, R., Ding, Q., Post, M., and Hui, C. C. (1998). Essential function of Gli2 and Gli3 in the formation of lung, trachea and oesophagus. *Nat. Genet.* **20,** 54–57.

Neubüser, A., Koseki, H., and Balling, R. (1995). Characterization and developmental expression of Pax9, a paired-box-containing gene related to Pax1. *Dev. Biol.* **170,** 701–716.

Noden, D. M. (1983). The role of the neural crest in patterning of avian cranial skeletal, connective, and muscle tissues. *Dev. Biol.* **96,** 144–165.

Ohkubo, Y., Chiang, C., and Rubenstein, J. L. (2002). Coordinate regulation and synergistic actions of BMP4, SHH and FGF8 in the rostral prosencephalon regulate morphogenesis of the telencephalic and optic vesicles. *Neuroscience* **111,** 1–17.

Porteus, M. H., Bulfone, A., Ciaranello, R. D., and Rubenstein, J. L. (1991). Isolation and characterization of a novel cDNA clone encoding a homeodomain that is developmentally regulated in the ventral forebrain. *Neuron* **7,** 221–229.

Ruiz i Altaba, A. (1999). Gli proteins and Hedgehog signaling development and cancer. *Trends Genet.* **15,** 418–425.

Sato, T., Araki, I., and Nakamura, H. (2001). Inductive signal and tissue responsiveness defining the tectum and the cerebellum. *Development* **128,** 2461–2469.

Shimamura, K., Hartigan, D. J., Martinez, S., Puelles, L., and Rubenstein, J. L. (1995). Longitudinal organization of the anterior neural plate and neural tube. *Development* **121,** 3923–3933.

St-Jacques, B., Dassule, H. R., Karavanova, I., Botchkarev, V. A., Li, J., Danielian, P. S., McMahon, J. A., Lewis, P. M., Paus, R., and

McMahon, A. P. (1998). Sonic hedgehog signaling is essential for hair development. *Curr. Biol.* **8,** 1058–1068.

Tanaka, A., Miyamoto, K., Minamino, N., Takeda, M., Sato, B., Matsuo, H., and Matsumoto, K. (1992). Cloning and characterization of an androgen-induced growth factor essential for the androgen-dependent growth of mouse mammary carcinoma cells. *Proc. Natl. Acad. Sci. USA* **89,** 8928–8932.

Theil, T., Alvarez-Bolado, G., Walter, A., and Rüther, U. (1999). Gli3 is required for Emx gene expression during dorsal telencephalon development. *Development* **126,** 3561–3571.

Theil, T., Aydin, S., Koch, S., Grotewold, L., and Rüther, U. (2002). Wnt and Bmp signalling cooperatively regulate graded Emx2 expression in the dorsal telencephalon. *Development* **129,** 3045–3054.

Tole, S., Ragsdale, C. W., and Grove, E. A. (2000). Dorsoventral patterning of the telencephalon is disrupted in the mouse mutant extra-toes(J). *Dev. Biol.* **217,** 254–265.

Trumpp, A., Depew, M. J., Rubenstein, J. L., Bishop, J. M., and Martin, G. R. (1999). Cre-mediated gene inactivation demonstrates that FGF8 is required for cell survival and patterning of the first branchial arch. *Genes Dev.* **13,** 3136–3148.

Walther, C., and Gruss, P. (1991). Pax-6, a murine paired box gene, is expressed in the developing CNS. *Development* **113,** 1435–1449.

Ye, W., Shimamura, K., Rubenstein, J. L., Hynes, M. A., and Rosenthal, A. (1998). FGF and Shh signals control dopaminergic and serotonergic cell fate in the anterior neural plate. *Cell* **93,** 755–766.

Received for publication March 4, 2002
Revised July 1, 2002
Accepted August 5, 2002
Published online October 10, 2002